# Modelling the Effect of Austenite Volume Fraction and Ferrite Particle Size on Mechanical Properties of Austempered Ductile Iron

**Jagmohan Datt[1] and Uma Batra[2]**

*[1,2]Deptt. of Materials and Metallurgical Engineering, PEC University of Technology, Chandigarh–160012*

*E-mail: [1]jdsharma@pec.ac.in*

**Abstract**—*Amongst the cast iron family, Austempered Ductile Iron (ADI) has a unique microstructure and an excellent, optimized combination of mechanical properties. The main microstructure of ADI is ausferrite, which is a mixture of extremely fine acicular ferrite and stable, high carbon austenite. There are two types of austenite in ADI: (i) the thin films of austenite between the individual ferrite platelets in the acicular structure and (ii) the coarser and more equi-axed blocks of austenite between non-parallel acicular structures. It is this unique microstructure, which gives ADI its excellent mechanical properties. The effect of microstructure on the mechanical properties is explained in detail by examining the structural parameters like austenite volume fraction and ferrite particle size. Mathematical relationships between mechanical properties and structural parameters have been established. ADI still has the potential to be further improved and its production and the number of applications for ADI will continue to grow, driven by the resultant cost savings over alternative materials.*

**Keywords:** *ADI; microstructure; mechanical properties; crystal structure; strengthening mechanism*

## Introduction

Austempered Ductile Iron (ADI) is recognized as an important engineering material because of its excellent mechanical properties including high strength, good ductility, good wear resistance and good fatigue strength [1-4]. The unique combination of ADIs properties has been attributed to the acicular morphology of ausferrite obtained by austempering. During austempering, the relatively high silicon contents present in nodular iron effectively hinder precipitation of carbide phases retaining relatively large amount of high carbon austenite. The high carbon austenite is thermally unstable and long austempering times promote it to decompose into ferrite and carbide. This reaction is undesirable as it leads to degradation of the exhibited properties, particularly the ADI toughness and ductility [1-9]. The addition of alloying elements can greatly affect the thermodynamics and kinetics of the phase transformation during austempering. The role of alloying elements on the reaction kinetics and microstructural stability at austempering temperature has been widely investigated [10]. The present investigation focuses on predicting the changes in mechanical properties that take place in unalloyed and nickel alloyed ADIs austempered at different temperatures. Relationships of strength and percent elongation of ADI have been established with austenite volume fraction, $X_\gamma$, and ferrite particle size, $d_\alpha$.

## Experimental Procedure

Two ductile irons of are produced in a commercial foundry using an induction melting furnace of medium high frequency. In present work, commercially viable ductile irons with minimum possible manganese content are produced. Cu and Ni are chosen to compensate for reduction in austemperability due to lowering of molybdenum and manganese contents. Copper and nickel, in contrast to molybdenum and manganese, does not segregate at cell boundaries and therefore supports uniformity in austempered structure. The ductile irons have following composition in wt%. Unalloyed ADI-0 : C = 3.59, Si = 2.71, Mg = 0.06, Mn = 0.35, Mo = 0.24, Cu = 0.6, S = 0.016, P = 0.018, Al = .02 and rest Fe. Alloyed ADI-6 is produced by adding 0.6wt% Ni in above composition.The molten metal was cast immediately in the shape of modified 2.5 cm (1-inch) Y-blocks shown in Fig. 2a. The qualitative and quantitative analysis of microstructure of the as-cast ductile iron (DI) was observed under optical microscope with Image Analyzer attachment (Carl Zeiss). The structural parameters of both DIs are presented in Table 1.

**Table 1: Structural and Mechanical Properties of DI**

| Property | DI-0 (Unalloyed) | DI-6 (Ni-alloyed) |
|---|---|---|
| Nodule count,$mm^{-2}$ | 200 | 180 |
| Nodule size, $mm^{-2}$ | 0.04 | 0.04 |
| Nodularity,% | 98 | 95 |
| Ferrite,% | 10 | 4 |
| Pearlite, % | 90 | 96 |
| Hardness, Hv10 | 270 | 208 |
| UTS, MPa | 711 | 740 |
| % El | 6.4 | 6.2 |

The tensile test specimens, in accordance with ASTM international specifications A 536-80, [11] were machined from the leg part of the Y-block castings. These sampleswere austenitized at 900°C for 120 minutes and transferred rapidly to a salt bath held at pre selected austempering temperature (270°C, 320°C, 370°C or 420°C) before quenching in water (Fig. 2b).

A pre-optimized austempering time of 120 minutes has been used so that the transformation of high carbon austenite to ferrite and carbide does not occur. Metallographic examination of ADI samples was carried

out using scanning electron microscopy (SEM, JEOL 840A). X-ray diffraction analysis (XRD, PW 1148/89) was performed on ADI samples using Cu Kα radiation (λ=1.54 Å) at 40 KV and 20 mA in 2θ range 40° to 93°, step size 0.1°, with count time of 2 seconds per step. The averages of amount of % vol of austenite, $X_\gamma$,and the effective "ferrite particle size" $d_\alpha$, in ausferrite product were estimated from XRD patterns for all ADIs under investigation following procedure described by Cullity [12]. Hardness of DI and ADI samples was measured using Vicker's Hardness Tester (IE make) with 10 kg load. Tensile tests were performed for DI and ADI samples on universal tensile testing machine of 20 tons capacity, UTS-20 (FI make) to estimate ultimate tensile strength (UTS), 0.2% proof strength ($\sigma_{0.2}$), and percent elongation (%El).

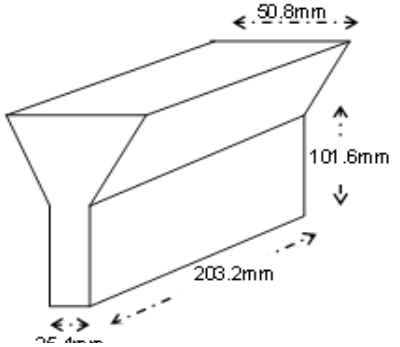


(a)

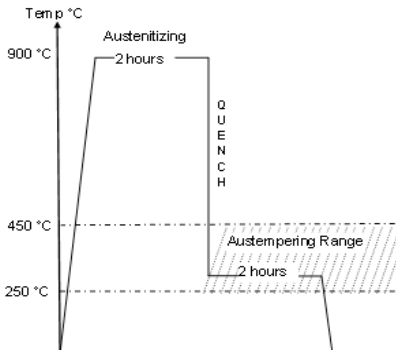


(b)

**Fig. 2:(a) Modified 1 inch 'Y' Block of Ductile Iron Castings, (b) Austempering Heat Treatment Cycle**

## Results and Discussion

### Microstructure

The SEM micrographs of ADI-6 austempered at 270°C, 320°C, 370°C, and 420°C are shown in Fig. 3. Both ADIs under investigations exhibit unique microstructure of ausferrite comprising of acicular ferrite and high carbon austenite.

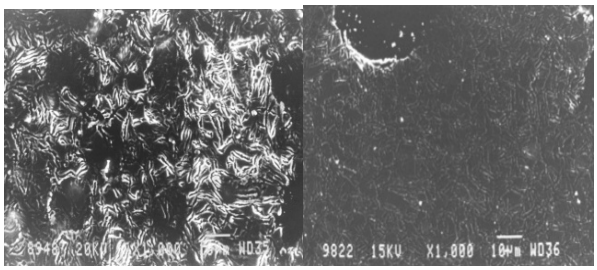


(a) (b)

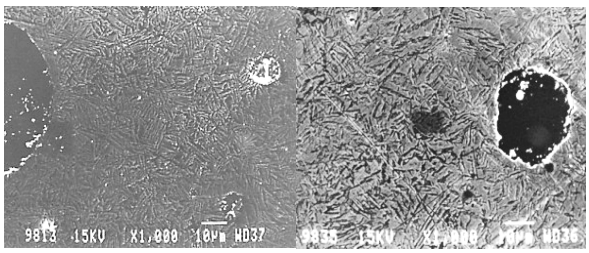


(c) (d)

**Fig. 3: Microstructure of ADI-6 Austempered at (a) 270°C (b) 320°C, (c) 370°C, & (d) 420°C**

Figure 3a shows microstructure of ADI-6, austempered at 270°C in which extremely fine ferrite plates are separated by thin films of high carbon austenite. The ferrite plates have grown in length as well as width in ADI-6 when austempered at 320°C (Fig. 3b). ADI-6 consists of more equiaxed blocks of austenite between non parallel "sheaves" of ferrite platelets when austempered at 370°C, and 420°C respectively shown in Fig. 3c and 3d. The variations in the microstructures of ADI-0 with austempering temperatures were similar to those observed in ADI-6.

### Structural Parameters & Mechanical Properties

The amount of vol% of austenite $X_\gamma$, and ferrite particle size $d_\alpha$ estimated from XRD patterns and the mechanical properties 0.2% proof strength, UTS, % elongation of ADIs is presented in Table 2. It is evident that $d_\alpha$ and $X_\gamma$ increase appreciably with rise in austempering temperature from 270°C to 420°C, and it is in agreement with the trend reported earlier [2, 5].

### Effect of Austempering Temperature on Mechanical Properties

#### *Hardness, 0.2% Proof Strength and UTS vs. Austempering Temperature, $T_A$*

Fig. 4a shows that the hardness decreases linearly with increasing austempering temperature for both the irons, in accordance with the coarsening of the ausferrite (Fig. 3 and Table 2).

**Table 2: The amount of Vol% of austenite $X_\gamma$, Ferrite Particle Size $d_\alpha$, Vicker Hardness $HV_{10}$, Proof Strength$_{0.2}$, and Tensile Strength UTS of ADIs' at Different Austempering Temperature ($T_A$)**

| ADI- | ADI-0 | | | | ADI-6 | | | |
|---|---|---|---|---|---|---|---|---|
| $T_A$, (°C) | 270 | 320 | 370 | 420 | 270 | 320 | 370 | 420 |
| $X_\gamma$ %Vol | 20 | 23 | 38 | 40 | 22 | 24 | 40 | 42 |
| $d_\alpha$, (Å) | 170 | 185 | 210 | 230 | 190 | 220 | 270 | 280 |
| $HV_{10}$ | 407 | 399 | 327 | 308 | 405 | 390 | 320 | 298 |
| $\sigma_{0.2}$, (MPa) | 860 | 810 | 750 | 683 | 896 | 850 | 790 | 740 |
| UTS, $10^9$ Pa | 1.11 | 1.08 | 0.99 | 0.93 | 1.07 | 1.04 | 0.95 | 0.91 |
| % El | 1.1 | 2.3 | 3.8 | 4.2 | 2.1 | 2.8 | 4.6 | 5.3 |

Figure 4b and 4c show that, similar tothe hardness dependence on $T_A$, the average 0.2% proof strength and UTS decreases with increasing austempering temperature. The higher value of tensile strength at lower temperature of austempering is also attributed to the finer size of ferrite needle, which makes matrix more uniform. The maximum strength values occurs at 270°C, because of presence of martensite at the intercellular regions due to lower diffusion rate of carbon and thus incomplete ausferrite transformation at lower temperature of austempering[2-4,9]. The hardness and strength decrease on increasing the austempering temperature. With the increase in temperature of austempering, the ausferrite become coarse and volume fraction of austenite in ausferrite increases, which are responsible for the decrease in hardness and strength.

## *% El vs. Austempering Temperature, $T_A$*

Figure 4d clearly shows that ADI displays only a marginal amount of increase in % elongation as the austempering temperature is increased. At 270°C, the percentage elongation is at a minimum due to finer ausferrite in the austempered structure and it increases appreciably on raising the austempering temperature to 420°C since the coarser ferrite and large quantity of blocky austenite is present [8]. At lower temperatures of austempering, the microstructure has untransformed austenite in intercellular region due to lower diffusion of carbon to the eutectic region. These region leads to martensitic transformation which adversely affects the % elongation of the material. As the temperature increases, the enhanced carbon diffusion leads to the stabilization of austenite even to the eutectic boundary region, which reduces the possibility of transformation of austenite to martensite. This leads to the increase in % elongation of the ADI with increasing austempering temperature.

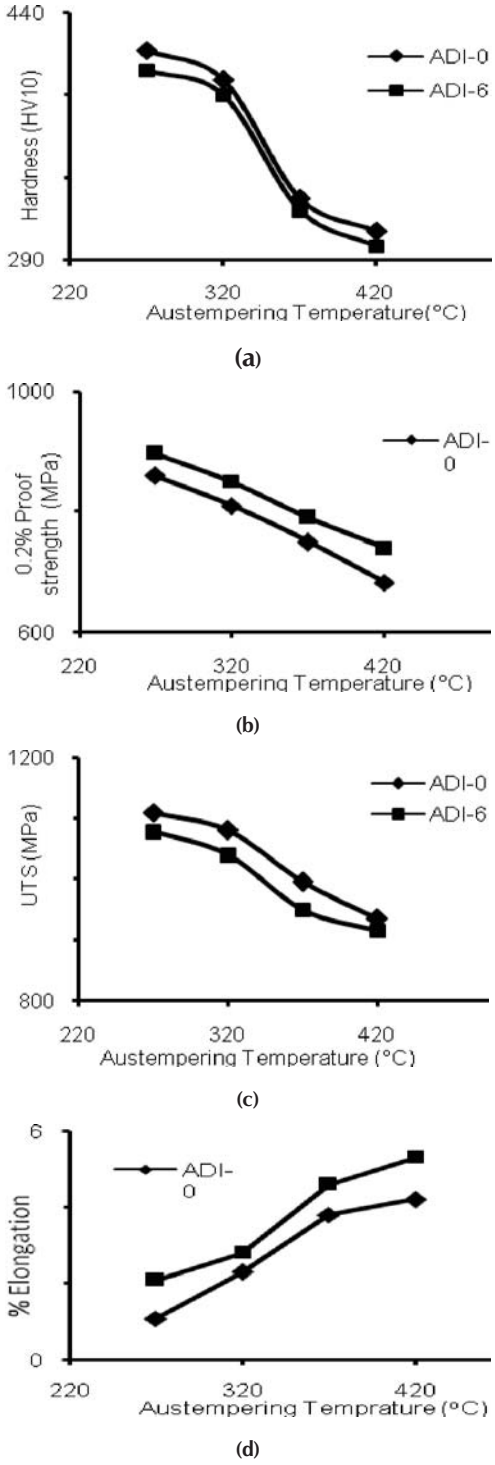


**Fig. 4: Effect of Austempering Temperature on (a) Hardness, Hv10; (b) 0.2% Proof Strength, MPa, and (c) UTS, MPa, (d) % Elongation**

## 0.2% Proof Strength & UTS vs. Hardness

Stress versus hardness behavior can be useful because it relates a mechanical property which requires a significant time commitment to obtain (strength) to a relatively easy measurement to record (hardness). An estimate of the UTS can then be interpolated from the hardness.

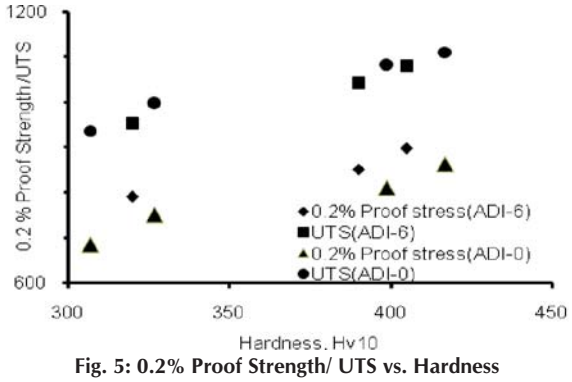


**Fig. 5: 0.2% Proof Strength/ UTS vs. Hardness**

## Effect of Matrix Microstructure on Mechanical Properties

Table 2 gives the averages of the austenite volume fractions and the effective "particle size", $d_\alpha$, of the ferrite in the ausferrite product measured by X-ray diffraction (XRD).

### *Effect of Austenite Fraction, $X_\gamma$ on Hardness, 0.2% Proof Strength, UTS and % Elongation*

Figures 6(a-c) illustrate plots of hardness, 0.2% Proof strength, UTS and % elongation vs. $X_\gamma$. It can be seen that, in general, the hardness, 0.2% Proof strength, and UTS decrease with increasing $X_\gamma$ and decreases with increasing $d_\alpha$ while the % elongation does the opposite, i,e. increase with increasing $X_\gamma$ and increases with increasing $d_\alpha$.The austenite volume fraction present in the ausferrite has a significant effect on the mechanical properties of ADI. From Fig. 6a the hardness decreases with an increasing volume fraction of austenite in the ausferrite product. This leads to the fact that austempering at lower temperatures will result in stronger components due in part to the ausferrite constituent containing less austenite. The amount of austenite present in the ausferrite product should also have a significant impact on the % elongation of this ADI.The data in Table 2 clearly show that the % elongation improves with increasing amounts of austenite from 1.1% for 270°C to as high as 4.2% total elongation for 420°C for ADI-0 and from 2.1% to 5.3% in ADI-6. Specimens have not been fully austempered at 270°C, and therefore, the intercellular regions contain some martensite. The graphitic structure will also determine the amount of elongation in ADIs.

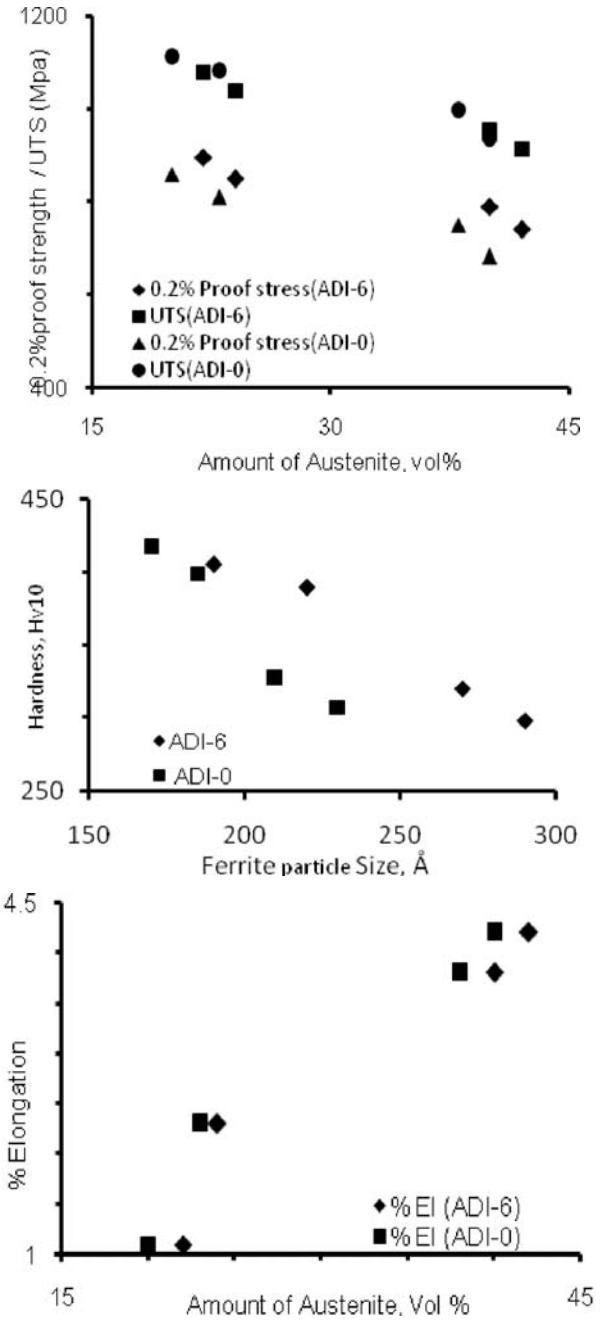


**Fig. 6: Effect of Austenite % Vol on the (a) Hardness, (b), 0.2% Proof Strength /UTS, (c) % Elongation**

### *Effect of Ferrite Particle Size, $d_\alpha$ on Hardness, 0.2% Proof Strength, UTS and % El*

Porosity or other casting related defects will also dramatically affect the elongation. No quantitative measurements were performed on the graphitic structure or the possible presence of defects during this study.

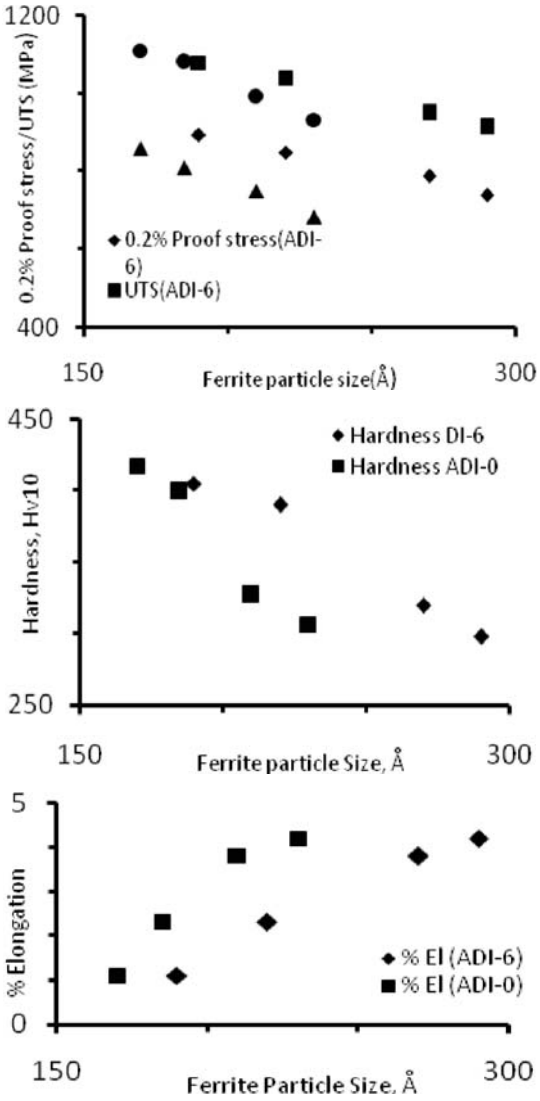


**Fig. 7: Effect of Ferrite Particle Size on the (a) 0.2% Proof Strength, UTS (b) Hardness, (c) % Elongation**

In addition to the amount of austenite in the ausferrite constituent, the size or scale of the ausferrite will also have a significant effect on the hardness, 0.2% Proof strength, UTS and % elongation of these ADIs.As might be expected, the 0.2% Proof strength, UTS and hardness increase (Fig. 7(a-b)) and % elongation decreases (Fig. 7c) with increasing fineness of the ausferrite. However, it should be noted that measuring the ferrite "particle size" based on the amount of XRD peak broadening has many inherent problems. In this case, the broadening which occurs has been attributed solely to a decreasing ferrite "particle size." In fact, there are other reason for XRD peak broadening most notably any strain present in the lattice from the casting process. Therefore, this analysis will predict a smaller particle size than actual but remains useful because the relative magnitudes should still follow in the same manner i,e. lower austempering temperature results a finer particle size.

## Modeling the Effects of Austenite Volume Fraction And Ferrite Particle Size on Mechanical Properties

The sensitivity that a mechanical property has on the on structural parameters, could be estimated by developing mathematical models exploring the dependence that hardness, 0.2% proof strength, UTS and % elongation on the austenite volume fraction, $X_\gamma$ and the ferrite particle size, $d_\alpha$, in the ausferrite product, which should display a Hall-Petch type relationship. Multilinear Regression (MLR) analyses were performed on the structural parameters and mechanical property data in given in Table 2 with exception of 270°C data.

$$HV10 = 328 + 2085 d\alpha^{-0.5} - 333 X_g \quad (2)$$

$$\sigma_y = 395 + 6617 d_\alpha^{-0.5} - 195 X_\gamma \quad (3)$$

$$UTS = 888.6 + 4065 d_\alpha^{-0.5} - 458 X_\gamma \quad (4)$$

$$\%El = -5.5 - 87.5 d_\alpha^{-0.5} + 11.6 X_g \quad (5)$$

The experimental models obtained from the MLR analyses are listed above with $d_\alpha$ in Angstroms and $X_\gamma$ being unit less.It is of particular interest to examine the coefficients in Eqs. 2-5 in view of the particular mechanical properties of hardness, % proof strength, tensile strength and % elongation. Equation 2 shows that the relative importance of the austenite volume fraction and ferrite particle size in determining the hardness is such that the particle size is relatively more important. Keeping in view that hardness test is essentially a compression test where the near continuity of the graphite is much less important than it is in tension. The presence of the soft graphite, by the rule of mixtures, only serves to diminish the hardness equally in all specimens because the graphite volume fraction remains relatively unchanged from one specimen to another. An increase in %vol of austenite in the amount observed in the experiment as the austempering temperature increases would, of itself, be expected to have only a small effect because austenite is only marginally softer than ferrite. In fact, Eq. 2 shows that increases in $X_\gamma$ will serve to slightly decrease the $HV_{10}$. Thus the chief contribution to the observed hardness change with heat treatment from the microstructural scale observed, it being much finer at low $T_A$ than at higher $T_A$. Fine ausferrite is expected to be much harder than coarse ausferrite.Equations 4 and 5, represents that 0.2% proof

strength and UTS, is quite similar to the $HV_{10}$ results (Eq. 4) in that the scale of the microstructure is the most important factor in determining the 0.2% proof strength and UTS. These findings are in good agreement with those of previous investigations for ADI those were developed from pure ductile iron and from those with Mn additions [3,7]. On the other hand, Eq. 5, representing % El, shows relative values of the coefficients describing the effect of $X_\gamma$ and $d_\alpha$ are much closer to one another, and that the effect of the austenite volume fraction is more important than particle size of the ferrite. This is intuitively correct because austenite is nominally more ductile than ferrite [13]. On the other hand the decreasing % elongation with decreasing particle size is a natural consequence of increasing strength observed in all engineering alloys.

## Conclusion

ADI has a unique microstructure of ausferrite, which is a mixture of acicular ferrite and stable, high carbon austenite. It is the extremely fine acicular ferrite, the high carbon thin films and the blocky austenite, which give ADI its excellent combination of strength, toughness, wear resistance and low temperature impact toughness. Considering the very fine scale of ausferrite, the unique microstructure, excellent mechanical properties and good castability, it can be concluded that there is still the potential to further improve ADI properties through tighter control of the casting, alloying addition and heat treatment processes to produce a microstructure that is much finer and more uniform. Modeling of the mechanical properties provide a useful tool to allow manufacture of ADI to produce the desired properties in particular components, with a significantly reduced number of experimental trials being necessary.

## References

[1] M. N. Ahmadabadi, H. M. Ghasemi, and M. Osia, "Effects of Successive Austempering on Tribological Behavior of DI," Wear, 1999, 231, pp. 293-300.

[2] K. L. Hayrynen, D. J. Moore, and K. B. Rundman, "Tensile and Fatigue Properties of Relatively Pure ADI, " Trans. AFS, 1992,100, pp. 93-104.

[3] T. N. Rouns, K. B. Rundman, and D. J. Moore, "On the Structure and Mechanical Properties of ADI, " Trans.AFS, 1984,92, pp. 815-40.

[4] T. S. Shih, C. S. Chang, and L. Z. Huang, "Mechanical Properties and Microstructures of ADI" Trans. AFS, 1991, 107, pp. 793-808.

[5] R. B. Gundlach, and J. F. Janowak, "Austempered Ductile Iron Combines Strength with Toughness and Ductility," Met. Prog.,July 1985,128, pp. 19-26.

[6] N. Darwish, and R. Elliot, "Austempering of Low Manganese Ductile Iron, Part 3. Variation of Mechanical Properties with Heat-Treatment Conditions,"Mater. Sci. Technol., 1993,9, pp.882-89.

[7] D. J. Moore, T. N. Rouns, and K. B. Rundman, "The Relationship between Microstructure and Tensile Properties in Austempered Ductile Iron," Trans. AFS, 1987,95, pp. 765-74.

[8] D. J. Moore, T. N. Rouns, and K. B. Rundman, "Structure and Mechanical Properties of Austempered DI" Trans. AFS, 1985, 93, pp. 705-18.

[9] U. Batra, S. Ray, and S. R. Prabhakar, "Austempering &ADIMicrostructure in Cu Alloyed DI," J. Mater. Eng. Perf.,2003, 112, pp. 426-29.

[10] D. Krishan Raj, H. N. L. Narasimhan and S. Seshan, Structure and Properties of Austempered Ductile Iron as Affected by Low Alloy Additions, Trans. AFS, 1992, 100, p 105-112.

[11] K. D. Mills,Spheroidal Graphite CI: Its Development & Future, Br. Foundryman, Vol 65, 1972, p 34.

[12] B. D. Cullity, Elements of X-ray Diffraction, Addison Wesley Publishing, 1956, pp. 390-396.

[13] W.F Smith, Structure and properties of engineering alloys, McGraw Hill, 1981.